

# Composite Fermions Waltz to the Tune of a Wigner Crystal

Yang Liu, H. Deng, M. Shayegan, L.N. Pfeiffer, K.W. West, and K.W. Baldwin  
*Department of Electrical Engineering, Princeton University, Princeton, New Jersey 08544*  
(Dated: March 14, 2022)

When the kinetic energy of a collection of interacting two-dimensional (2D) electrons is quenched at very high magnetic fields so that the Coulomb repulsion dominates, the electrons are expected to condense into an ordered array, forming a quantum Wigner crystal (WC). Although this exotic state has long been suspected in high-mobility 2D electron systems at very low Landau level fillings ( $\nu \ll 1$ ), its direct observation has been elusive. Here we present a new technique and experimental results that directly probe the magnetic-field-induced WC. We measure the magneto-resistance of a bilayer electron system with unequal layer densities at high magnetic fields. One layer has a very low density and is in the WC regime ( $\nu \ll 1$ ), while the other ("probe") layer is near  $\nu = 1/2$  and hosts a sea of composite fermions, quasi-particles formed by attaching two flux-quanta to each interacting electron. The composite fermions feel the periodic electric potential of the WC in the other layer and exhibit magneto-resistance maxima whenever their cyclotron orbit encircles certain integer number of the WC lattice points. The positions of the maxima reveal that the WC has a triangular lattice and yield a direct measure of its lattice constant. Our results provide a striking example of how one can probe an exotic many-body state of 2D electrons using equally exotic quasi-particles of another many-body state.

Interacting two-dimensional (2D) electrons subjected to high perpendicular magnetic fields ( $B$ ) and cooled to low temperatures exhibit a plethora of exotic quasi-particles and states [1–3]. At  $\nu = 1/2$  Landau level filling factor, for example, the interacting electrons capture two flux-quanta each and create new quasi-particles, called composite fermions (CFs) [3–5]. The CFs offer an elegant explanation for the fractional quantum Hall effect (FQHE) [6]. Furthermore, because of the flux attachment, the effective magnetic field ( $B_{eff}$ ) felt by the CFs vanishes at  $\nu = 1/2$  so that CFs occupy a Fermi sea and exhibit Fermi-liquid-like properties, similar to their zero-field electron counterparts [3, 5, 7–13]. In particular, in the presence of an imposed periodic potential, the resistance of the CFs oscillates as a function of  $B_{eff} = B - B_{1/2}$ , where  $B_{1/2}$  is the value of the external field at  $\nu = 1/2$  [8–13]. These oscillations are a signature of the commensurability of the CFs' quasi-classical cyclotron orbit diameter with an integer multiple of the period of the imposed potential, and their positions in  $B_{eff}$  are directly related to the symmetry and period of the potential.

Another example of a collective state is the Wigner crystal (WC) [14], an ordered array of electrons, believed to form at very small fillings ( $\nu \ll 1$ ) when the Coulomb repulsion between electrons dominates [15–25]. The WC, being pinned by the ubiquitous residual disorder, manifests as an insulating phase in DC transport [18, 20, 21, 23], and exhibits resonances in its AC (microwave) transport which strongly suggest collective motions of the electrons [22, 24, 25]. So far, however, there have been no direct measurements of the WC order or its lattice constant.

Here we present high magnetic field data in bilayer electron systems where one layer has a very low density and is in the WC regime, while the adjacent layer is near

$\nu = 1/2$  and contains CFs (Fig. 1(a)). The data exhibit commensurability oscillations in the magneto-resistance of the CF layer, induced by the periodic potential of WC electrons in the other layer (Fig. 1(b)), and provide a unique glimpse at the symmetry of the WC and its lattice constant.

Our samples were grown via molecular beam epitaxy and consist of two, 30-nm-wide, GaAs quantum wells (QWs) separated by an undoped  $\text{Al}_{0.24}\text{Ga}_{0.76}\text{As}$  barrier layer whose thicknesses are 10 and 50 nm. The QWs are modulation-doped with Si  $\delta$ -layers asymmetrically: the bottom QW has a 300-nm-thick spacer layer while the spacer for the top QW is 80 nm thick. This asymmetry leads to very different as-grown 2D electron densities in the QWs; the top layer has a density of  $n_T \approx 1.4 \times 10^{11} \text{ cm}^{-2}$ , which is much higher than the bottom layer density  $n_B \approx 0.4 \times 10^{11} \text{ cm}^{-2}$ . Based on the growth parameters and our data in other, single-layer samples, we expect both layers to have very high quality. Our estimated low-temperature mobility for the top layer is  $\approx 10^7 \text{ cm}^2/\text{Vs}$ , and for the bottom layer  $\approx 10^6 \text{ cm}^2/\text{Vs}$ . The samples are  $4 \times 4 \text{ mm}^2$ , with InSn contacts at their four corners, and are fitted with an In back-gate which covers the entire back surface of the wafer. Applying a negative voltage bias ( $V_{BG}$ ) to this back-gate reduces  $n_B$ . The measurements were carried out in a dilution refrigerator with a base temperature of  $\sim 25 \text{ mK}$ , and using low-frequency ( $\leq 40 \text{ Hz}$ ) lock-in technique.

The longitudinal resistance ( $R_{xx}$ ) vs magnetic field ( $B$ ) data presented in Fig. 2 capture the highlight of our findings. The data are shown only in the high- $B$  region of interest. The traces are for the bilayer sample at different  $V_{BG}$  to decrease  $n_B$ . In the bottom trace, taken at a large negative  $V_{BG}$ , the bottom layer is essentially depleted so that the trace represents  $R_{xx}$  for the top layer. This trace exhibits the usual characteristics seen in high-

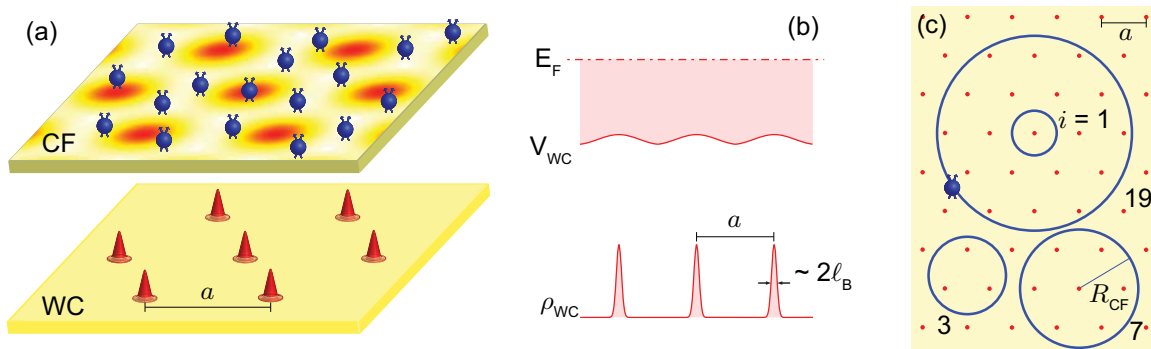


FIG. 1. Overview of our measurements. (a) Our bilayer system has a high-density top layer which hosts a CF Fermi sea at high magnetic fields near its filling factor  $\nu_T = 1/2$ . The bottom layer has a much lower density so that it is at a very small filling factor ( $\nu_B \ll 1$ ), thus allowing a WC to form. (b) The top layer feels a periodic potential modulation  $V_{WC}$  from the bottom WC layer's charge density  $\rho_{WC}$ ;  $l_B$  is the magnetic length. (c) As the magnetic field is swept near top-layer's  $1/2$  filling, the CFs in the top layer execute cyclotron motion, leading to commensurability maxima in the magneto-resistance of the top layer when the CF cyclotron orbit encircles 1, 3, 7, 19,  $\dots$  lattice points.

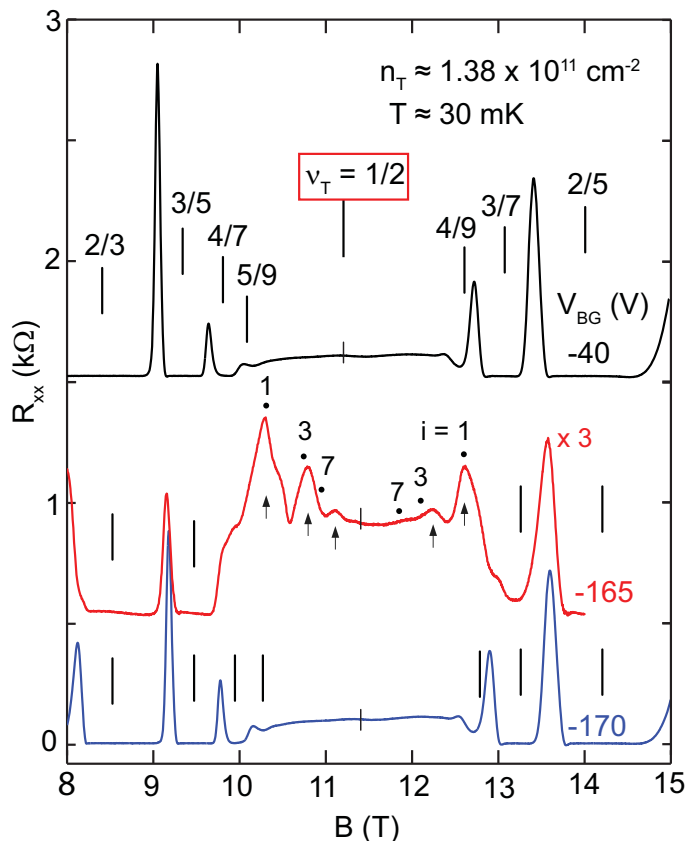


FIG. 2.  $R_{xx}$  vs.  $B$  traces for the 50-nm-barrier sample, measured as the bottom-layer density is reduced via applying negative back-gate voltage.

quality 2D electron systems:  $R_{xx}$  has minima at numerous odd-denominator fillings such as  $2/3$ ,  $3/5$ , etc., indicating FQHE states, and is essentially flat and featureless close to  $\nu_T = 1/2$ . The features in the top trace, which is taken at a small negative  $V_{BG}$ , are also characteristic

of a simple, single-layer 2D electron system. They, too, essentially reflect the properties of the top layer, including its density and filling factors as a function of  $B$ , as indicated in Fig. 2. The bottom layer, although present, is at a reasonably small filling factor ( $\nu_B \leq 1/6$ ), has very high resistance, and appears not to contribute to  $R_{xx}$  at high fields. The middle trace in Fig. 2 which is taken just before the bottom layer is depleted, however, is unusual. Its density and filling factors are clearly those of the top layer, but near  $\nu_T = 1/2$  there are oscillatory features that are superimposed on a larger background (compared to the top and bottom traces). As we discuss in the remainder of our manuscript, these strong oscillations near  $\nu_T = 1/2$  reflect the commensurability of the cyclotron orbits of the CFs in the top layer with the periodic electric potential induced by a WC formed in the bottom layer (see Fig. 1).

To test our hypothesis, we carefully analyze the positions of the anomalous  $R_{xx}$  maxima observed near  $\nu_T = 1/2$  in the middle trace of Fig. 2. We associate the two  $R_{xx}$  peaks observed farthest from  $\nu_T = 1/2$ , namely those at  $B \approx 10.3$  and  $12.6$  T, with the primary commensurability condition when the CF cyclotron orbit diameter ( $2R_{CF}$ ) equals the period ( $a$ ) of the WC lattice ( $i = 1$  circle in Fig. 1(c)). The primary  $R_{xx}$  maximum on the right side of  $B_{1/2}$  is slightly farther from  $B_{1/2}$  ( $B_{eff} = B - B_{1/2} \approx 1.20$  T) compared to the maximum on the left side ( $B_{eff} \approx -1.13$  T). This asymmetry and its approximate magnitude ( $\sim 5\%$ ) are consistent with the asymmetries reported recently in CF commensurability data obtained with an imposed unidirectional periodic potential [13]. Using the relation  $R_{CF} = \hbar k_{CF} / eB_{eff}$ , where  $k_{CF} = \sqrt{4\pi n_{CF}}$  is the CF Fermi wavevector and  $n_{CF}$  is the density of CFs [26], and  $n_T \approx 1.38 \times 10^{11} \text{ cm}^{-2}$ , we find  $R_{CF} \approx 70$  nm on both sides, implying a WC period  $a \approx 140$  nm, or WC density  $n_{WC} \approx 6 \times 10^9 \text{ cm}^{-2}$ .

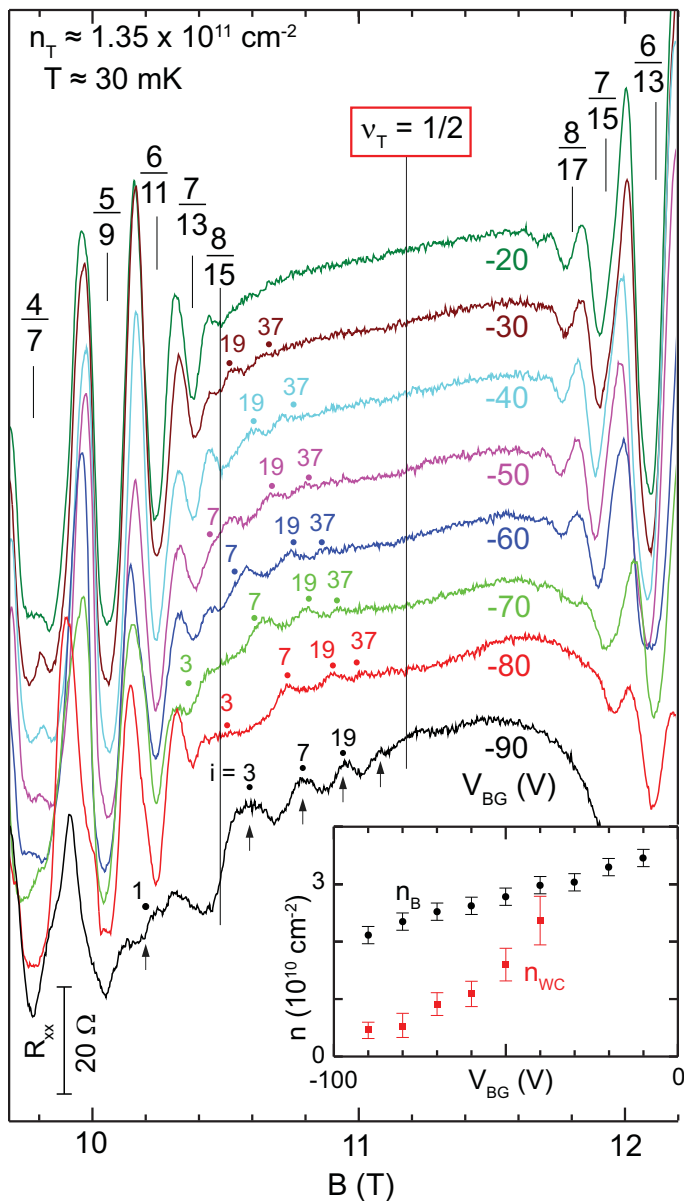


FIG. 3.  $R_{xx}$  vs.  $B$  traces for the 10-nm-barrier sample near  $\nu_T = 1/2$  as the bottom-layer density is slowly decreased via applying more negative  $V_{BG}$ . The commensurability oscillations are seen on the left side of  $\nu_T = 1/2$ . They move away from  $\nu_T = 1/2$  as  $V_{BG}$  and the WC density ( $n_{WC}$ ) increases and, for  $\nu_T > 8/15$  ( $B \leq 10.5$  T), are masked by the strong FQHE minima (see, e.g., the lowest three traces). Inset: The red square symbols show  $n_{WC}$  deduced from the commensurability oscillations at each  $V_{BG}$ , and the black circles indicate the expected bottom-layer density  $n_B$  near  $\nu_T = 1/2$ .

Several aspects of the Fig. 2 data are consistent with associating the  $R_{xx}$  features in the range  $10 < B < 13$  T with a WC. First, the amplitudes of the  $R_{xx}$  maxima are larger on the left side of  $B_{1/2}$ . This is consistent with data reported for CFs moving in a 2D periodic potential [8–10], specially when the potential is shallow so that the CFs do not encircle fully depleted regions

(anti-dots) in the sample [9, 10]. Second, for a triangular lattice, expected for a spin-polarized WC, the CF commensurate orbits should encircle 1, 3, 7, 19, ... lattice points (see Fig. 1(c)), implying that  $B_{eff}$  positions of the higher-order  $R_{xx}$  peaks should ideally have ratios of  $(1 : 1/\sqrt{3} : 1/\sqrt{7} : 1/\sqrt{19} : \dots) \approx (1 : 0.577 : 0.378 : 0.229 : \dots)$ . In Fig. 2 these expected positions, marked with small circles, are reasonably consistent with the observed positions of  $R_{xx}$  maxima although there are clear discrepancies for the weak maxima. Third, a trace taken at a higher temperature of 0.3 K in a similar sample and under similar conditions exhibits strong FQHE states but not the  $R_{xx}$  maxima near  $\nu_T = 1/2$ , suggesting a melting of the WC.

Data taken on a similar bilayer sample but with a 10-nm-thick barrier between the two QWs corroborate our conclusions (Fig. 3). Here we show the evolution of  $R_{xx}$  traces as we gradually increase  $n_B$  by applying less negative biases to the back-gate [27]. In the lowest trace  $n_B$  is quite small [28], and we observe pronounced oscillations on the left side of  $\nu_T = 1/2$ . Associating the  $R_{xx}$  maxima with the commensurability of CF cyclotron orbits with a periodic potential, we find that the data are remarkably consistent with a triangular lattice of period  $\approx 160$  nm, or  $n_{WC} \approx 5 \times 10^9$  cm $^{-2}$ . As seen in Fig. 3, the small circles, which indicate the expected positions of  $R_{xx}$  maxima for CF orbits that encircle 1, 3, 7 and 19 lattice points in such a lattice (see Fig. 1(c)), indeed match the observed  $R_{xx}$  maxima very well. As  $V_{BG}$  is made less negative and the top-layer density is increased in Fig. 3, the  $R_{xx}$  maxima seen to the left of  $\nu_T = 1/2$  move to lower magnetic fields, away from  $\nu_T = 1/2$ , and are eventually engulfed by the top layer's strong FQHE features. This movement is consistent with the maxima stemming from a WC whose density increases, as expected when  $V_{BG}$  is increased to raise  $n_B$ . We believe that the data in Fig. 3, and particularly the lowest trace, provide clear evidence that the CFs in the top layer are indeed dancing to the tune of a WC formed in the bottom layer.

An intriguing finding in our experiments is that the WC density ( $n_{WC}$ ) we deduce from the high-field commensurability data is typically smaller than our expected  $n_B$ . In our measurements, the Fourier transform of the Shubnikov-de Haas oscillations at very low fields ( $B \leq 0.7$  T) exhibits two peaks whose frequencies directly yield  $n_B$  and  $n_T$ . We find that  $n_T$  is in excellent agreement with the top-layer density at high fields, deduced from the positions of the FQHE minima near  $\nu = 1/2$ , provided we take into account a small charge transfer ( $\delta n \approx 4 \times 10^9$  cm $^{-2}$ ) that occurs from the bottom to the top layer at intermediate magnetic fields [29]. Based on the same charge transfer model, or by simply subtracting  $n_T$  at high fields from the total density of the system, we find that our  $n_B$  at high fields is significantly larger than  $n_{WC}$ . For the middle trace in Fig. 2, e.g., in the high-field regime we expect  $n_B \approx 1.2 \times 10^{10}$  cm $^{-2}$ ,

which is larger than  $n_{WC} \approx 6 \times 10^9 \text{ cm}^{-2}$  deduced from the positions of  $R_{xx}$  maxima near  $\nu_T = 1/2$  by a factor of  $\approx 2$ . This discrepancy is also seen in Fig. 3 inset, where we compare the deduced  $n_{WC}$  (red squares) to the expected  $n_B$  at high field (black circles). The source of these discrepancies is unclear. We believe it is unlikely that they stem from uncertainties in our estimate of the densities. It is more likely that the number of electrons forming the WC in the bottom layer is less than the total number of electrons in this layer. The remainder of the electrons might be localized at high magnetic fields by the random disorder potential, and serve to screen this potential. It is worth emphasizing that knowing the number of WC electrons in DC experiments is indeed very challenging even in single-layer systems. Deep in the WC regime ( $\nu \ll 1$ ), the system is insulating at low temperatures as the 2D electrons are pinned, and there are no features from which one can deduce the density. In AC (microwave resonance) experiments, an estimate of  $n_{WC}$  can be made from the strength of the resonance [24]. It was indeed reported that  $n_{WC}$  can be smaller than the expected layer density [24], but there are uncertainties from the background signal and the model used to interpret the data. From this perspective, our technique and data demonstrate a means for directly determining the density of electrons that form the WC via measuring the WC lattice constant.

Our results are likely to stimulate work in several areas. For example, what is the exact shape of the periodic potential modulation that the WC layer imposes on the CFs? A related question is the optimum shape and magnitude of the periodic potential, and the interlayer distance that would lead to the most pronounced  $R_{xx}$  commensurability maxima. The answer could also explain why the data for the sample with a 50-nm-thick interlayer barrier (Fig. 2) show strong  $R_{xx}$  maxima on both sides of  $\nu_T = 1/2$  while the sample of Fig. 3, whose barrier is only 10 nm thick, exhibits numerous maxima but only on the left side of  $\nu_T = 1/2$ . Considering previous studies of CF commensurability features in 2D periodic arrays [8–10], it is very likely that this asymmetry betrays the soft and shallow potential that the WC electrons impose on the CFs, but a quantitative link is missing.

More generally, the weak periodic potential imposed by the WC and the homogeneous *effective* magnetic field  $B_{eff}$  can conspire to also lead to a fractal energy diagram (the Hofstadter’s butterfly) [30] for the of CFs, similar to what has been studied for *electrons* in an externally imposed periodic potential [31, 32]. The WC electrons might also modify other properties of CFs. For example, a fully spin-polarized WC can enhance the degree of spin-polarization of CFs. In our measurements we do indeed observe hints of this, as the FQHE states in the top layer appear to become more easily polarized in our bilayer system compared to a single-layer system. Finally, our technique might find use in studying other possibly

ordered, broken-symmetry states of 2D carrier systems. For example, we envision measurements where the CFs in one layer are used to probe, in an adjacent layer, the anisotropic phases that are observed at half-filled Landau levels with high index [33–35]. These anisotropic phases are believed to signal many-body states, consisting of stripes of electrons with alternating density (filling). If the stripes are periodic, they would generate a one-dimensional periodic potential in the nearby CF layer, and the CFs should exhibit commensurability features.

We acknowledge support through the NSF (DMR-1305691) for measurements, and the Gordon and Betty Moore Foundation (Grant GBMF4420), Keck Foundation, the NSF MRSEC (DMR-0819860), and the DOE BES (DE-FG02-00-ER45841) for sample fabrication.

- 
- [1] *Perspectives in Quantum Hall Effects*, edited by S. D. Sarma and A. Pinczuk (Wiley, New York, 1998).
  - [2] M. Shayegan, in *High Magnetic Fields*, edited by F. Herlach and N. Miura (World Scientific, Singapore, 2006), pp. 31–60.
  - [3] J. K. Jain, *Composite Fermions* (Cambridge University Press, Cambridge, UK, 2007).
  - [4] J. K. Jain, *Phys. Rev. Lett.* **63**, 199 (1989).
  - [5] B. I. Halperin, P. A. Lee, N. Read, *Phys. Rev. B* **47**, 7312 (1993).
  - [6] D. C. Tsui, H. L. Stormer, A. C. Gossard, *Phys. Rev. Lett.* **48**, 1559 (1982).
  - [7] R. L. Willett, R. R. Ruel, K. W. West, L. N. Pfeiffer, *Phys. Rev. Lett.* **71**, 3846 (1993).
  - [8] W. Kang, H. L. Stormer, L. N. Pfeiffer, K. W. Baldwin, K. W. West, *Phys. Rev. Lett.* **71**, 3850 (1993).
  - [9] J. H. Smet, *et al.*, *Phys. Rev. B* **56**, 3598 (1997).
  - [10] J. H. Smet, K. von Klitzing, D. Weiss, W. Wegscheider, *Phys. Rev. Lett.* **80**, 4538 (1998).
  - [11] D. Kamburov, *et al.*, *Phys. Rev. Lett.* **110**, 206801 (2013).
  - [12] D. Kamburov, *et al.*, *Phys. Rev. B* **89**, 085304 (2014).
  - [13] D. Kamburov, *et al.*, *arXiv:1406.2379* (2014); *Phys. Rev. Lett.* (in press).
  - [14] E. Wigner, *Phys. Rev.* **46**, 1002 (1934).
  - [15] Y. Lozovik, V. Yudson, *JETP Lett.* **22**, 11 (1975).
  - [16] P. K. Lam, S. M. Girvin, *Phys. Rev. B* **30**, 473 (1984).
  - [17] D. Levesque, J. J. Weis, A. H. MacDonald, *Phys. Rev. B* **30**, 1056 (1984).
  - [18] For a review, see M. Shayegan, in Ref. [1]; pp. 343–383.
  - [19] E. Y. Andrei, *et al.*, *Phys. Rev. Lett.* **60**, 2765 (1988).
  - [20] H. W. Jiang, *et al.*, *Phys. Rev. Lett.* **65**, 633 (1990).
  - [21] V. J. Goldman, M. Santos, M. Shayegan, J. E. Cunningham, *Phys. Rev. Lett.* **65**, 2189 (1990).
  - [22] F. I. B. Williams, *et al.*, *Phys. Rev. Lett.* **66**, 3285 (1991).
  - [23] Y. P. Li, T. Sajoto, L. W. Engel, D. C. Tsui, M. Shayegan, *Phys. Rev. Lett.* **67**, 1630 (1991).
  - [24] C.-C. Li, L. W. Engel, D. Shahar, D. C. Tsui, M. Shayegan, *Phys. Rev. Lett.* **79**, 1353 (1997).
  - [25] Y. P. Chen, *et al.*, *Phys. Rev. Lett.* **93**, 206805 (2004).
  - [26] We use  $n_{CF} = n_T$  for  $B_{eff} > 0$  and  $n_{CF} = \frac{1-\nu}{\nu} n_T$  for  $B_{eff} < 0$ , namely we assume that  $n_{CF}$  is equal to

the minority carriers density in the lowest Landau level of the top layer; see Ref. [13]. If we assume a constant density for CFs,  $n_{CF} = n_T$ , we also obtain similarly good agreement to within  $\leq 5\%$  between the observed and expected positions of the resistance maxima.

- [27] In Fig. 3,  $n_T$  slightly changes for each 10-V-step of increasing  $V_{BG}$ . The  $B$ -axis is only for the bottom trace, and the other traces are scaled accordingly in order to match the top layer filling factors.
- [28] Unfortunately, we could not lower the back-gate in this sample below -90 V.
- [29] The origin of the charge transfer is the mismatch between the ground-state energies of the two layers that have unequal densities but are in thermal equilibrium, and the requirement that the lowest Landau levels of the two layers have to align at high magnetic fields when both layers

are in the extreme quantum limit. In a simple, capacitive model, the magnitude of the charge transferred from the bottom to the top layer is  $\delta n = (n_T - n_B) \cdot \frac{\pi \hbar^2}{m^*} \cdot \frac{1}{\epsilon d}$ , where  $d$  is the distance between the charge distribution peaks of the two layers.

- [30] D. R. Hofstadter, *Phys. Rev. B* **14**, 2239 (1976).
- [31] C. Albrecht, *et al.*, *Phys. Rev. Lett.* **86**, 147 (2001).
- [32] S. Melinte, *et al.*, *Phys. Rev. Lett.* **92**, 036802 (2004).
- [33] M. P. Lilly, K. B. Cooper, J. P. Eisenstein, L. N. Pfeiffer, K. W. West, *Phys. Rev. Lett.* **82**, 394 (1999).
- [34] R. R. Du, *et al.*, *Solid State Communications* **109**, 389 (1999).
- [35] M. Shayegan, H. Manoharan, S. Papadakis, E. Poortere, *Physica E: Low-dimensional Systems and Nanostructures* **6**, 40 (2000).